JFM RAPIDS
journals.cambridge.org/rapids

Thermal delay of drop coalescence

Michela Geri[1], Bavand Keshavarz[1], Gareth H. McKinley[1]
and John W. M. Bush[2],†

[1]Department of Mechanical Engineering, Massachusetts Institute of Technology, Cambridge,
MA 02139, USA

[2]Department of Mathematics, Massachusetts Institute of Technology, Cambridge, MA 02139, USA

We present the results of a combined experimental and theoretical study of drop coalescence in the presence of an initial temperature difference ΔT_0 between a drop and a bath of the same liquid. We characterize experimentally the dependence of the residence time before coalescence on ΔT_0 for silicone oils with different viscosities. Delayed coalescence arises above a critical temperature difference ΔT_c that depends on the fluid viscosity: for $\Delta T_0 > \Delta T_c$, the delay time increases as $\Delta T_0^{2/3}$ for all liquids examined. This observed dependence is rationalized theoretically through consideration of the thermocapillary flows generated within the drop, the bath and the intervening air layer.

Key words: breakup/coalescence, Marangoni convection, thermocapillarity

1. Introduction

When a drop falls onto a bath of a miscible liquid, one expects it to coalesce immediately upon impact. However, such is not always the case, owing to the presence of a thin lubricating air layer between drop and bath that must drain to a critical thickness before coalescence is initiated by intermolecular forces (Walker 1978). Careful observation of raindrops hitting a puddle, lake or sea surface reveal that some millimetric droplets may bounce, leap and roll along the surface prior to coalescence (Reynolds 1881; Rayleigh 1899). Everyday experience indicates that a temperature difference may further delay coalescence. When milk is poured into hot tea or coffee, drops may linger on the surface, levitating there for up to a few seconds before merging.

Coalescence has been studied extensively and the influence of relevant physical quantities (fluid density ρ, surface tension σ, viscosity μ, surface charges, etc.) has been characterized (e.g. Charles & Mason 1960*a,b*; Jeffreys & Davis 1971), leading to a classification of different dynamical regimes (Aryafar & Kavehpour 2006). Advances
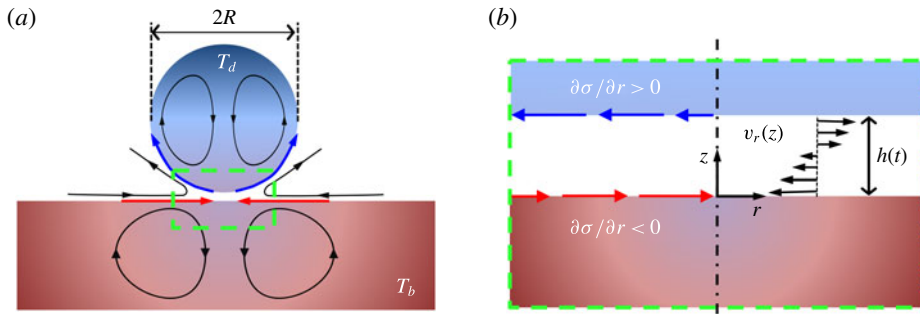
† Email address for correspondence: bush@math.mit.edu

M. Geri, B. Keshavarz, G. H. McKinley and J. W. M. Bush

FIGURE 1. A schematic of thermally delayed drop coalescence. (*a*) A drop approaches a bath of the same liquid with initial temperature difference $\Delta T_0 = T_b - T_d$. Thermal gradients induce Marangoni stresses that drive thermocapillary flows within both the liquid and gas phases. (*b*) A close-up of the lubrication layer of air between drop and bath.

in high-speed imaging (Thoroddsen & Takehara 2000), experimental techniques (Mohamed-Kassim & Longmire 2004), and numerical simulations (Blanchette & Bigioni 2006, 2009) have furthered our understanding of coalescence in various circumstances, including the effects of concentration-induced Marangoni stresses (Blanchette, Messio & Bush 2009). The myriad aspects of coalescence were recently reviewed by Kavehpour (2015).

The influence of thermal effects on drop coalescence has received relatively less attention. A series of experimental studies have examined the non-coalescence of two drops maintained at different temperatures owing to the presence of thermally induced Marangoni stresses (Dell'Aversana, Banavar & Koplik 1996; Dell'Aversana, Tontodonato & Carotenuto 1997; Dell'Aversana & Neitzel 1998). These studies demonstrate that above a critical temperature difference, coalescence is precluded by Marangoni stresses driving recirculating flows inside the drops that enhance the intervening lubrication pressure (as in figure 1) – a physical picture supported by the numerical simulations of Monti, Savino & Cicala (1996) and Monti & Savino (1997). Savino, Paterna & Lappa (2003) confirmed that coalescence of drops floating on a liquid bath could be delayed by a temperature difference between drop and bath, and the sustenance of the intervening air film by the associated thermocapillary flows. Neitzel & Dell'Aversana (2002) and Lappa (2005) have reviewed studies of different aspects of non-coalescence.

While it has been established that the influence of thermocapillary flows in the lubricating air layer will resist coalescence between two drops with a temperature difference above some critical value (Neitzel & Dell'Aversana 2002; Savino *et al.* 2003), no theoretical model has provided a rationale for this critical temperature difference. Moreover, previous studies have neither characterized nor rationalized the dependence of the residence time of a floating droplet (denoted τ_r henceforth) on the temperature difference between drop and bath. We focus here on the coalescence of a drop into a bath of the same liquid, when an initial temperature difference ΔT_0 is imposed between the bath and the drop (figure 1*a*). In §2 we provide experimental evidence of a functional relationship between τ_r and ΔT_0. In §3, we rationalize our observations through theoretical consideration of the thermocapillary flows arising within the drop, the bath and the intervening air layer.
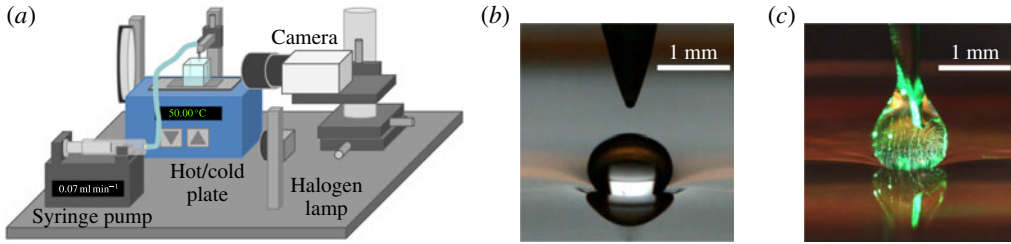
FIGURE 2. (*a*) Schematic of the experimental set-up. (*b*) Image showing a drop sitting on a bath of 1 cSt silicone oil with $\Delta T_0 = 0$ prior to coalescence (see movie 1). (*c*) Image captured with a green laser light sheet reveals a recirculating Marangoni flow within a cold drop (see movie 2).

2. Experiments

Consider a drop with initial temperature T_d approaching a bath of the same liquid with temperature T_b (figure 1*a*). The drop is released sufficiently close to the bath surface that the effect of its initial velocity is negligible. The initial temperature difference between the drop and the bath, $\Delta T_0 = T_b - T_d$, is prescribed. Owing to the dependence of surface tension σ on temperature T, thermal gradients along the interface result in Marangoni stresses that drive thermocapillary flows within both the liquid and gas phases, of the general form sketched in figure 1. The majority of our experiments were performed with $\Delta T_0 > 0$, as in the case of a cold milk drop on the surface of hot coffee. We also performed several experiments with $\Delta T_0 < 0$.

2.1. *Materials and methods*

Figure 2(*a*) shows a schematic of our experimental set-up. The bath consists of a liquid pool in a customized square cell of dimensions 3.175 cm by 3.175 cm by 1.9 cm deep. The cell, with acrylic walls and a metallic substrate, is placed on a dual cold/hot plate (Teca AHP-301 CPV) that allows for precise control of the temperature at the base of the cell. The temperature of the bath surface (T_b) and that of the drop (T_d) are monitored with a hand-held thermometer equipped with a K-type thermocouple. In the range of ΔT_0 considered, the influence of convective overturning within the bath was negligible. Drops are dispensed through a needle centred above the cell at a height of approximately one drop diameter above the bath. The liquid is pushed by a syringe pump at a flow rate of 0.07 ml min^{-1}, the drop then gently released onto the bath in order to insure a negligible approach speed. A BD stainless steel standard bevel needle 16G was used, fixing the drop radius to be $R = 0.6$ mm. A Phantom high-speed camera, mounted on a 3-axis positioning stage, recorded each experiment, typically at 2000 f.p.s. Figure 2(*b*) shows a digital video frame of a drop floating on a bath prior to coalescence (see movie 1 as a supplementary material available online at https://doi.org/10.1017/jfm.2017.686). Back-lighting with a white LED was used in all measurements (see movie 3), but a halogen lamp proved more effective in visualizing the rapid dynamics of the coalescence process, as shown in figure 3 (see also movies 4 and 5). The residence time τ_r was measured as the interval between drop detachment from the needle and the onset of coalescence (see first two images in figure 3*a,b*), which is readily identified by the appearance of capillary waves on the surface of the droplet. The acquisition rate guarantees that the error on τ_r is on the order of 1 ms, and so negligible relative to the variability between successive measurements.
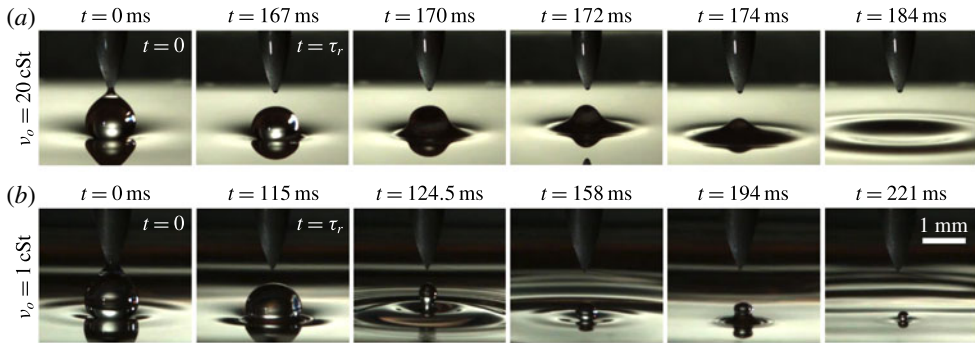
FIGURE 3. Montage of typical experiments for two different silicone oils with kinematic viscosities (*a*) $\nu_o = 20$ cSt and (*b*) $\nu_o = 1$ cSt (see also movies 4 and 5). The first two frames correspond to drop detachment from the needle ($t = 0$) and initiation of coalescence ($t = \tau_r$). Subsequent images show the coalescence process. The difference between the two sequences is striking: the 20 cSt drop coalesces directly, while the 1 cSt drop executes a coalescence cascade (Thoroddsen & Takehara 2000) with up to five to six daughter droplets, only two of which are shown here.

In order to visualize the thermocapillary flow within the drop, the 5 cSt oil was seeded with TiO_2 particles with an average diameter of 3 µm. A drop was then formed, pinned in place by the dispensing needle and illuminated with a green laser sheet (see movie 2). A synthetic streak image obtained by superposing 100 digital video frames taken at 30 f.p.s. prior to coalescence is shown in figure 2(*c*). The particle pathlines are clearly evident and reveal a poloidal motion with characteristic speed of ~ 5 mm s^{-1} in the interior of the drop for $\Delta T_0 = 5\,°C$. This vortical circulation is initiated when the droplet detaches from the needle (see movie 2). A complementary thermocapillary flow is expected to arise within the bath (Savino *et al.* 2003, see figure 1).

Silicone oils allowed us to tune viscosity without substantially altering other properties of the liquid phase (see table 1 in Kavehpour, Ovryn & McKinley 2002). Five different silicone oils were tested, with kinematic viscosities (ν_o) of 1, 5, 10, 20 and 500 cSt. All the oils are assumed to have density $\rho_o = 0.9$ g cm^{-3} and thermal diffusivity $\alpha_o = 7 \times 10^{-4}$ cm^2 s^{-1}. The surface tension is assumed to decrease linearly with increasing temperature: $\sigma(T) = \sigma_0 - \sigma_T(T - T_0)$ where $\sigma_0 = 20$ dyn cm^{-1} and $\sigma_T = \partial\sigma/\partial T = 5 \times 10^{-2}$ dyn (cm°C)$^{-1}$. The air is characterized by its dynamic viscosity $\mu_a = 0.018$ cP, density $\rho_a = 1.2 \times 10^{-3}$ g cm^{-3} and thermal diffusivity $\alpha_a = 0.2$ cm^2 s^{-1}. In our theoretical developments, density and viscosity are assumed to be independent of temperature: the only property that changes significantly over the range of temperatures considered is surface tension.

2.2. *Measurements of the residence time*

In figure 4(*a*) we report the residence times τ_r for the five oils at different ΔT_0. The dashed line indicates the isothermal reference value that is independent of the oil viscosity and assumes a nearly constant value $\tau_r^0 \simeq 160 \pm 50$ ms for all liquids considered and for the given R. Two important features should be noted. First, as in the case of complete non-coalescence of drops (Dell'Aversana *et al.* 1996), there is a critical temperature difference below which the residence time τ_r is comparable to
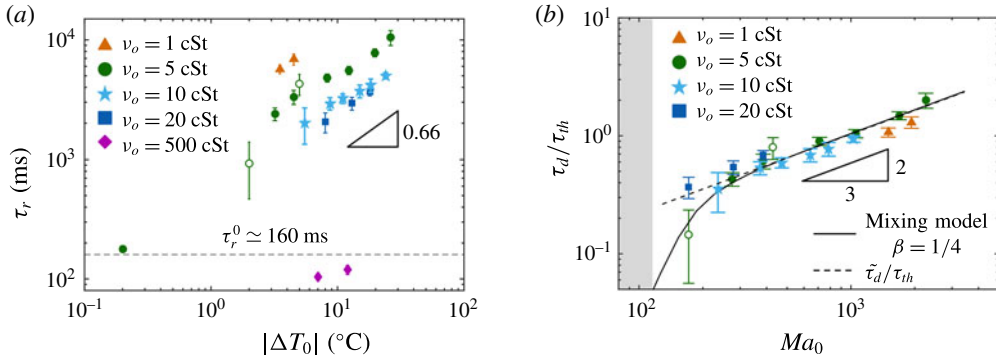
FIGURE 4. (*a*) Measurements of the residence time τ_r as a function of the absolute value of the initial temperature difference $|\Delta T_0|$ for the five different silicone oils considered. Open symbols represent the cases where $\Delta T_0 < 0$. Each data point corresponds to an average over 30 drops and error bars are equivalent to two standard deviations. (*b*) The delay time τ_d, non-dimensionalized by the characteristic thermal diffusion time $\tau_{th} = R^2/\alpha_o$, as a function of the initial Marangoni number Ma_0. Symbols correspond to data from (*a*). The solid line is the theoretical prediction from the model described in §3.2 with $\beta = 1/4$. The dashed line is an approximate closed-form expression derived in the limit of $t > \sqrt{3}/\dot{\gamma}$.

τ_r^0, as indicated by the points lying close to the reference dashed line. This critical value, henceforth denoted ΔT_c, increases monotonically with the fluid viscosity. While the 5 cSt oil has $\Delta T_c \simeq 1\,^\circ\text{C}$, the 500 cSt oil has a value of ΔT_c much higher than those accessible with our set-up; thus we never observed delayed coalescence with this oil. Second, above ΔT_c, for all viscosities the residence time monotonically increases with the initial temperature difference with a characteristic power law such that $\tau_r \sim \Delta T_0^{0.66 \pm 0.10}$.

To isolate the influence of thermocapillary flows, we introduce the delay time $\tau_d = \tau_r - \tau_r^0$ and rescale the initial temperature difference in terms of the initial Marangoni number $Ma_0 = |\Delta\sigma_o|R/\mu_o\alpha_o = |\sigma_T\Delta T_0|R/\mu_o\alpha_o$, which prescribes the relative magnitudes of the characteristic time scales of thermal diffusion and convection within the drop – respectively, $\tau_{th} = R^2/\alpha_o$ and $\tau_{conv} = R\mu_o/(\sigma_T\Delta T_0)$. In figure 4(*b*) we recast the data of figure 4(*a*) in terms of these two variables, with the delay time non-dimensionalized by the characteristic thermal diffusion time τ_{th}. The data all collapse onto a single curve that approaches a line with slope $2/3$ at large Ma. We note that the threshold below which no delayed coalescence is observed, previously characterized in terms of a viscosity-dependent ΔT_c, may now be expressed in terms of a single critical Marangoni number, $Ma_c \simeq 100 \pm 50$. Consequently, the delay time may be expressed as $\tau_d/\tau_{th} \simeq 0.01(Ma_0 - Ma_c)^{2/3}$. We also note that the points in figure 4(*a*) with $\tau_r \sim \tau_r^0$ are automatically shifted to $Ma \ll Ma_c$ and so are beyond the limits of the plot. In order to rationalize both Ma_c and the resulting power law scaling of τ_d with Ma, we proceed by considering the thermocapillary flows generated within the system.

3. Theoretical modelling

In §3.1, we first describe the air flow in the gap between the drop and the bath using a lubrication analysis from which the critical Marangoni number Ma_c is deduced.

In § 3.2, we then rationalize the functional relationship between the residence time and the initial temperature difference through a description of the mixing dynamics within the drop.

3.1. *Lubrication flow within the air gap*

Our analysis rests on a series of simplifying assumptions. Figure 2(*b,c*) suggest that the geometry of the flow is non-trivial due to the bath curvature induced locally by the drop's weight. Previous studies (Dell'Aversana *et al.* 1997; Neitzel & Dell'Aversana 2002; Savino *et al.* 2003) have pointed out that in these conditions the underside of the drop may deform such that the height of the gap is not constant. We avoid such geometrical complexities by treating the gap as a cylindrical disk with height $h(t)$ and radius R_d, where $R_d = R^2/l_c$ is the effective contact radius (Mahadevan & Pomeau 1999), and $l_c = \sqrt{\sigma/\rho_o g}$ is the capillary length of the oil; an approximation one expects to be valid provided $Bo = \rho_o g R^2/\sigma < 1$. In our experiments $Bo = 0.17$ and $R_d = 0.25$ mm $\simeq 0.4R$. The initial height of the gap is $h(0)$ and $h(t) \ll (R, R_d)$ at all times.

We also assume that $Re_a(h/R) \ll 1$, where $Re_a = \rho_a V h_0/\mu_a$ is the Reynolds number of the air flow, so that the lubrication approximation can be invoked and the Navier–Stokes equations simplified to:

$$0 \simeq -\frac{\partial p}{\partial r} + \mu_a \frac{\partial^2 v_r}{\partial z^2}, \quad 0 \simeq -\frac{\partial p}{\partial z}, \quad (3.1a,b)$$

where p is the pressure field and v_r the radial velocity. While both boundaries are free, $\mu_o/\mu_a \gg 1$ so we can apply no-slip boundary conditions, specifically $v_r(0) = v_b$, the surface speed of the bath, and $v_r(h(t)) = v_d$, the surface speed of the drop. Note that v_b and v_d can be positive or negative depending on the sign of ΔT_0. If $\Delta T_0 > 0$, $v_b < 0$ while $v_d > 0$, and *vice versa* (see figure 1). In isothermal conditions, one may assume that $v_b = 0 = v_d$, and the problem reduces to the classic lubrication squeezing flow between two parallel disks (Stefan 1874). However, in the presence of thermal gradients, both interfaces have radial flows driven by Marangoni stresses with characteristic magnitude $U_0 \sim \sigma_T \Delta T/\mu_o$, leading to the following mixed Couette–Poiseuille velocity profile within the gap:

$$v_r(r, z) = \frac{1}{2\mu_a} \left(-\frac{\partial p}{\partial r} \right) [zh - z^2] + (v_d - v_b)\frac{z}{h} + v_b. \quad (3.2)$$

After imposing conservation of mass for a control volume within the gap and the kinematic boundary condition $v_z = -\dot{h}$ at $z = h$, one can use the velocity profile to derive an ordinary differential equation (ODE) for the pressure field:

$$-\frac{\partial p}{\partial r} = \frac{6\mu_a(-\dot{h})}{h^3}r + \frac{6\mu_a \Delta v}{h^2}, \quad (3.3)$$

where $\Delta v = -(v_d + v_b) > 0$ regardless of the sign of ΔT_0 (Monti *et al.* 1996). Integrating (3.3) with the boundary condition $p(R_d) = p_a$ yields:

$$p(r) - p_a = \frac{3\mu_a(-\dot{h})}{h^3}(R_d^2 - r^2) + \frac{6\mu_a \Delta v}{h^2}(R_d - r). \quad (3.4)$$

The form of the pressure field indicates that the Marangoni flow augments the pressure within the gap, thus resisting the settling of the drop, independent of the sign of ΔT_0. Assuming that the drop acceleration is negligible, so that its weight is supported quasistatically by the pressure field, we deduce:

$$\rho_o \frac{4}{3}\pi R^3 g = 2\pi \int_0^{R_d} [p(r) - p_a] r \, dr = \frac{3\pi\mu_a R_d^4}{2h^3}(-\dot{h}) + \frac{2\pi\mu_a R_d^3 \Delta v}{h^2}. \qquad (3.5)$$

We thus obtain an ODE for the height of the gap $h(t)$. We define a dimensionless height $h^\star = h/h_0$, and a dimensionless time $t^\star = t/\tau_s$, where $\tau_s = 9\mu_a R_d^4/(16\rho_o g R^3 h_0^2)$ is the characteristic settling time that would arise in the absence of thermocapillary effects. A balance between thermocapillary and viscous stresses at the interface allows us to express Δv as $\Delta v = K|\sigma_T \Delta T|/\mu_o$, with $K \sim O(1)$. In the absence of direct measurements of the surface velocity, we set the constant K to unity. We thus write the ODE in dimensionless form as:

$$-\frac{\partial h^\star}{\partial t^\star} = h^\star \left(\frac{h^{\star 2}}{2} - \frac{4}{3}\frac{\tau_s}{\tau_{th}}\frac{R}{R_d} Ma \right), \qquad (3.6)$$

where $\tau_{th} = R^2/\alpha_o$ is the thermal diffusion time and $Ma = |\sigma_T \Delta T|R/\mu_o \alpha_o$ is the Marangoni number. Under isothermal conditions ($Ma = 0$), equation (3.6) yields the well-known solution $h^\star(t^\star) = 1/\sqrt{1 + t^\star}$ for squeezing flow between two disks under constant force (Stefan 1874).

If $Ma \neq 0$, equation (3.6) indicates that there is a critical value Ma_c above which the gap height does not decrease in time. Using values of fluid properties listed in §2.1 and an estimated initial height of $h_0 = 1.5$ µm (Monti & Savino 1997) we obtain $\tau_s = 0.0078$ s and $\tau_{th} = 5.14$ s, which gives $Ma_c = 3\tau_{th}R_d/(8\tau_s R) \simeq 100$, in good agreement with the experimental results. The value of Ma_c can be used to estimate ΔT_c for any viscosity. In particular, for $\nu_o = 5$ cSt the critical temperature difference is $\Delta T_c = Ma_c \mu_o \alpha_o/\sigma_T R \simeq 1\,°C$, in agreement with our experiments, while for $\nu_o = 500$ cSt, $\Delta T_c \simeq 115\,°C$, which is well beyond the maximum accessible ΔT_0 and so again consistent with our experiments. We further note that the exact value of Ma_c depends on the quantities h_0 and K, which have only been estimated here. Precise measurements of both would be required for a more accurate estimate of Ma_c.

3.2. *Mixing and its effect on the residence time*

The flow induced by Marangoni stresses acting on the air within the gap accounts for the existence of a critical Marangoni number. To rationalize the dependence of the thermal delay time on ΔT_0, we need to estimate the time required for such stresses to diminish, i.e. for temperature differences to decrease such that $Ma < Ma_c$. Formally, this requires the combined solution of the energy equation and the Navier–Stokes equations. However, a relatively expedient route may be found with appropriate simplifications.

Figure 2(c) provides direct evidence of convection and the resulting thermal homogenization by highlighting the recirculating flow inside the drop prior to coalescence. Assuming that the characteristic velocity is that of the interface $U_0 \sim |\sigma_T \Delta T_0|/\mu_o$, one obtains an estimate of the convective time scale $\tau_{conv} \sim R/U_0 \sim R\mu_o/|\sigma_T \Delta T_0| \sim \tau_{th}/Ma_0$. Given that $Ma_0 \geqslant Ma_c \simeq 100$, we infer that $\tau_{conv} \ll \tau_{th}$ so that convection dominates in the initial stages of thermalization. This suggests that when the drop gets close to the bath its lower extremities are warmed up (or cooled
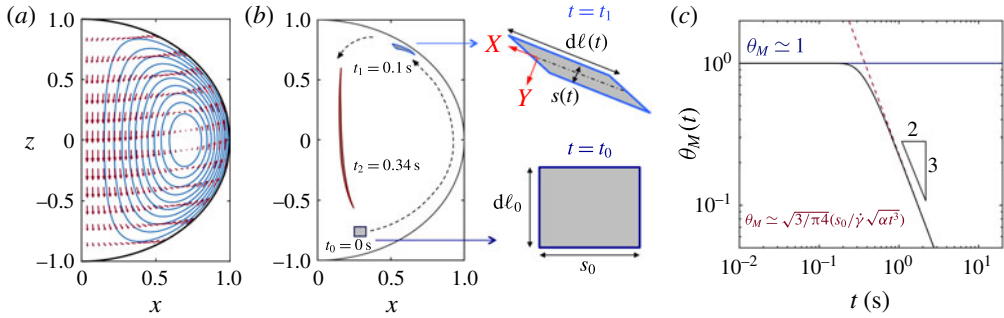
FIGURE 5. (a) Streamlines (blue) and velocity field (red) of the potential flow solution corresponding to Hill's spherical vortex. (b) Simulation of a fluid element being deformed and convected with the assumed potential flow (with $\Delta T_0 = 10\,^\circ\text{C}$, $\nu_o = 5$ cSt, see also movie 6). The accompanying schematic indicates the reference system of (3.9). (c) Predicted decay of temperature obtained through (3.12) for $\Delta T_0 = 26\,^\circ\text{C}$ and $\nu_o = 5$ cSt (solid black line). Approximation of the solution for early times ($t \to 0$, solid blue line) and for long times ($t > \sqrt{3}/\dot{\gamma}$, dashed red line).

down, depending on the sign of ΔT_0) and a poloidal convective motion is established that rapidly transports these fluid elements while deforming them into elongated filaments, or lamellae. Only on longer time scales does thermal diffusion become effective and the drop equilibrate thermally.

A mathematical framework to study related advection–diffusion problems has been developed in the context of mixing by Ottino, Ranz & Macosko (1979) and Ranz (1979), and recently applied by Meunier & Villermaux (2003) to describe scalar mixing in an axisymmetric vortex flow. In the following, we apply this method to the case of thermal homogenization within the drop, assuming that a roughly symmetric process is also taking place in the bath (Savino *et al.* 2003). We assume that the velocity field is expressible in terms of the Hill's spherical vortex (Batchelor 1967, p. 237). Defining a dimensionless velocity field as $\boldsymbol{v}^\star = \boldsymbol{v}/\bar{U}$, where $\bar{U}$ is a characteristic velocity proportional to U_0 and a dimensionless radial coordinate as $r^\star = r/R$, the dimensionless velocity components for this potential flow are $v_r^\star = -(1 - r^{\star 2})\cos\theta$ and $v_\theta^\star = (1 - 2r^{\star 2})\sin\theta$, which are plotted together with the streamlines ($\psi^\star = 1/2(r^{\star 2} - 1)r^{\star 2}\sin^2\theta = $ const.) in figure 5(a). From these expressions, we compute the dimensionless strain rate tensor within the drop:

$$\boldsymbol{e}^\star = \begin{pmatrix} 2r^\star\cos\theta & -3/2r^\star\sin\theta \\ -3/2r^\star\sin\theta & -r^\star\cos\theta \end{pmatrix}. \tag{3.7}$$

Accounting for the evident spatial variations would substantially complicate the analysis; hence, we consider an average flow by performing an area-weighted average of the local shear rate tensor over all angles θ in the range $[0, \pi]$, obtaining

$$\langle \boldsymbol{e}^\star \rangle = \frac{1}{\pi}\int_0^\pi \int_0^1 \boldsymbol{e}^\star r^\star \, d\theta \, dr^\star = \begin{pmatrix} 0 & -1/\pi \\ -1/\pi & 0 \end{pmatrix}. \tag{3.8}$$

Equation (3.8) suggests that, on average, each element of fluid undergoes a shearing deformation. To find the dimensional average shear rate $\dot{\gamma}$ we consider

833 R3-8

the shear rate at the interface to be that imposed by the gradient in surface tension, $\dot{\gamma}_R = (\partial\sigma/\partial\theta)/2\mu_o R = |\sigma_T \Delta T|/2R\pi\mu_o$. Computing the maximum shear rate at the interface ($r^\star = 1$, $\theta = \pi/2$) from (3.7), we deduce $\bar{U} = U_0/3\pi$ and $\dot{\gamma} = U_0/(3\pi^2 R)$. Following the method introduced by Ottino *et al.* (1979), we write the energy equation in the frame of reference (X, Y) of a material element that is convected and deformed as shown in figure 5(*b*). Neglecting variations in the X-direction, we write:

$$\frac{\partial T}{\partial t} + V\frac{\partial T}{\partial Y} = \alpha_o \frac{\partial^2 T}{\partial Y^2}. \tag{3.9}$$

The velocity field V can be written in terms of the thickness of the lamella $s(t)$ based on the rate of stretching $\dot{\epsilon} = \mathrm{d}\ln s(t)/\mathrm{d}t$ as $V = \dot{\epsilon}Y$. For a flow dominated by shear, $s(t) = s_0/\sqrt{1 + \dot{\gamma}^2 t^2}$, where s_0 is the initial size of the blob of fluid that has been warmed up (or cooled down) to a temperature close to T_b as the drop approaches the bath. An estimate of s_0 can be derived by considering that convection can be induced only when a temperature gradient is established on the drop surface. Consequently, s_0 is prescribed by the local balance, at early times, between diffusion from the bath, at a rate $\alpha_o/(\mathrm{d}\ell)^2$ with $\mathrm{d}\ell \sim \sqrt{\alpha_o t}$ independent of the temperature difference, and deformation by Marangoni stresses, at a rate $|\sigma_T \Delta T_0|/(\mu_o s_0)$. When $|\sigma_T \Delta T_0|/(\mu_o s_0) \geqslant \alpha_o/(\mathrm{d}\ell)^2$, that is for $s_0 \simeq Ma_0(\mathrm{d}\ell)^2/R$, the fluid blob will start moving. As convection is established, this initial blob of fluid at $T \sim T_b$ is stretched into a thin lamella that is wrapped around the drop (see movie 6). Ultimately, the drop is characterized by a series of alternating warm and cold layers.

By changing variables such that $\xi = Y/s(t)$ and $\tau = \int_0^t \alpha_o/s^2(t')\,\mathrm{d}t'$, we can reduce (3.9) to:

$$\frac{\partial\theta}{\partial\tau} = \frac{\partial^2\theta}{\partial\xi^2}, \tag{3.10}$$

where $\theta = (T_b - T)/\Delta T_0$ and $\xi \in [-1/2, 1/2]$. The change of variables effectively rescales the convection–diffusion equation in order to capture the correct length and time scales over which thermalization acts, specifically those of a stretching and thinning lamella. By definition, convection dominates diffusion when $\tau \ll 1$. As τ approaches $O(1)$, the two become comparable so that conduction across the lamella becomes important.

To characterize the thermal equilibration of the drop, we solve (3.10) from the perspective of a lamella originally at T_d, in contact at its boundaries with fluid at T_b. In terms of dimensionless quantities this means that $\theta(\tau = 0) = 1$ inside the lamella (for $|\xi| < 1/2$), and $\theta(\tau = 0) = 0$ outside (for $|\xi| > 1/2$). The resulting analytical solution of (3.10) thus emerges:

$$\theta(\xi, \tau) = \frac{1}{2}\left[\mathrm{erf}\left(\frac{\xi + 1/2}{2\sqrt{\tau}}\right) - \mathrm{erf}\left(\frac{\xi - 1/2}{2\sqrt{\tau}}\right)\right]. \tag{3.11}$$

From (3.11) we can compute the evolution of the maximum temperature difference arising at the centre of the lamella $\xi = 0$:

$$\theta_M(0, t) = \frac{\Delta T_{lamella}(t)}{\Delta T_0} = \mathrm{erf}\left(\frac{1}{4\sqrt{\tau(t)}}\right) = \mathrm{erf}\left(\frac{s_0}{4\sqrt{\alpha_o t + \alpha_o \dot{\gamma}^2 t^3/3}}\right). \tag{3.12}$$

Equation (3.12) is plotted in figure 5(*c*) for the case of $\Delta T_0 = 26\,^\circ\mathrm{C}$ and $\nu_o = 5$ cSt. The temperature difference is initially constant since fluid elements are first convected

and deformed into lamellae before diffusion becomes significant. When $4\sqrt{\tau} \sim 1$, thermal diffusion acts effectively across the thickness of the lamella, altering the local temperature and ultimately leading to thermal homogenization of the drop. At long times (3.12) shows that $\Delta T(t)_{lamella} \sim \Delta T_0 \sqrt{3/(4\pi\alpha_o)}(s_0/(\dot{\gamma}t^{3/2}))$. This suggests that the delay time should scale as $\tau_d \sim \Delta T_0^{2/3} \sim Ma_0^{2/3}$. We note that the same scaling applies provided the kinematics of the flow field do not have elongational characteristics such that fluid elements separate exponentially quickly in time.

Using (3.12) for a fixed viscosity, we can obtain an estimate for the delay time as a function of ΔT_0. We expect the temperature difference across a lamella before coalescence (at $t \simeq \tau_d$) to be comparable to the critical temperature difference measured for the entire drop at uniform temperature, i.e. $\Delta T_{lamella}(\tau_d) = \beta \Delta T_c$ with $\beta \sim O(1)$. The resulting estimate for the delay time τ_d obtained by solving this nonlinear equation is shown in figure 4(*b*) with a solid curve computed with $\beta = 1/4$. Comparison with the data shows that, notwithstanding the simplifying assumptions, our analytical model effectively captures the main physical phenomena, rationalizing the observed dependence of τ_d on Ma_0. Finally, we note that a closed form for τ_d can be obtained from $\Delta T_{lamella}(\tau_d) = \beta \Delta T_c$ in the limit $t > \sqrt{3}/\dot{\gamma}$. In this case we have $\tilde{\tau}_d = (\sqrt{3}\Delta T_0 s_0/(\sqrt{4\pi\alpha_o}\beta\Delta T_c\dot{\gamma}))^{2/3}$, as shown as a dashed line in figure 4(*b*). As $Ma_0 \to Ma_c$, this approximation is no longer valid because it is based on the neglect of the linear term in t in (3.12) that becomes significant for small $\dot{\gamma}$.

4. Summary and conclusions

We have investigated the role of temperature differences between drop and bath in delaying drop coalescence. Experiments indicate a minimum temperature difference, dependent on the oil viscosity, below which no appreciable difference with the isothermal case exists and above which the residence time increases as a function of the initial temperature difference. We have demonstrated that the observed behaviour is described by a unique curve: above a critical Marangoni number Ma_c the delay time τ_d increases as $\tau_d/\tau_{th} \sim (Ma_0 - Ma_c)^{2/3}$.

By analysing the lubrication air flow within the gap, we have shown that the critical Marangoni number is prescribed by the minimum velocity that must be established for the pressure field, induced by the recirculating air flow within the gap, to sustain the drop's weight. Due to the symmetry of the pressure field, the effect is independent of the sign of ΔT_0, as indicated by our experiments. By considering the kinematics of thermal mixing in a frame deforming with the fluid elements, we have calculated the characteristic time scale for thermal homogenization within the drop, rationalizing the observed dependence of τ_d on Ma_0 (and therefore on ΔT_0).

Our study suggests that a similar formulation can be applied to the case of drop flotation (Savino *et al.* 2003) and also to the case of impinging drops (Dell'Aversana *et al.* 1996) provided the drop weight is replaced by the applied load. The onset of the coalescence cascade should be delayed but otherwise largely unaffected by an initial temperature difference between the mother droplet and the bath. Once the first drop has coalesced, following the thermal mixing process elucidated here, the temperature of its daughter droplets should be comparable to that of the bath. Finally, we note that thermally delayed drop coalescence may prove useful in levitating drops on vibrating baths (Bush 2015).

Acknowledgements

Initiative and Chevron ETC. M.G. thanks Professor A. E. (Peko) Hosoi for her encouragement and enthusiasm.

Supplementary movies

Supplementary movies are available at https://doi.org/10.1017/jfm.2017.686.

References

ARYAFAR, H. & KAVEHPOUR, H. P. 2006 Drop coalescence through planar surfaces. *Phys. Fluids* **18** (7), 072105.

BATCHELOR, G. K. 1967 *An Introduction to Fluid Dynamics*. Cambridge University Press.

BLANCHETTE, F. & BIGIONI, T. P. 2006 Partial coalescence of drops at liquid interfaces. *Nat. Phys.* **2**, 254–257.

BLANCHETTE, F. & BIGIONI, T. P. 2009 Dynamics of drop coalescence at fluid interfaces. *J. Fluid Mech.* **620**, 333–352.

BLANCHETTE, F., MESSIO, L. & BUSH, J. W. M. 2009 The influence of surface tension gradients on drop coalescence. *Phys. Fluids* **21** (7), 072107.

BUSH, J. W. M. 2015 Pilot-wave hydrodynamics. *Annu. Rev. Fluid Mech.* **47**, 269–292.

CHARLES, G. E. & MASON, S. G. 1960a The coalescence of liquid drops with flat liquid/liquid interfaces. *J. Colloid Sci.* **15**, 236–267.

CHARLES, G. E. & MASON, S. G. 1960b The mechanism of partial coalescence of liquid drops at liquid/liquid interfaces. *J. Colloid Sci.* **15**, 105–122.

DELL'AVERSANA, P., BANAVAR, J. R. & KOPLIK, J. 1996 Suppression of coalescence by shear and temperature gradients. *Phys. Fluids* **8** (1), 15–28.

DELL'AVERSANA, P. & NEITZEL, G. P. 1998 When liquids stay dry. *Phys. Today* 38–41.

DELL'AVERSANA, P., TONTODONATO, V. & CAROTENUTO, L. 1997 Suppression of coalescence and of wetting: the shape of the interstitial film. *Phys. Fluids* **9** (9), 2475–2485.

JEFFREYS, G. V. & DAVIS, G. A. 1971 Coalescence of liquid droplets and liquid dispersion. In *Recent Advances in Liquid–Liquid Extraction*, chap. 14, pp. 495–584. Pergamon.

KAVEHPOUR, H. P. 2015 Coalescence of drops. *Annu. Rev. Fluid Mech.* **47** (1), 245–268.

KAVEHPOUR, H. P., OVRYN, B. & MCKINLEY, G. H. 2002 Evaporatively-driven Marangoni instabilities of volatile liquid films spreading on thermally conductive substrates. *Colloids Surf.* A **206** (1–3), 409–423.

LAPPA, M. 2005 Coalescence and non-coalescence phenomena in multi-material problems and dispersed multiphase flows: part 2, a critical review of CFD approaches. *Fluid Dyn. Mater. Process.* **1** (3), 213–234.

MAHADEVAN, L. & POMEAU, Y. 1999 Rolling droplets. *Phys. Fluids* **11** (9), 2449.

MEUNIER, P. & VILLERMAUX, E. 2003 How vortices mix. *J. Fluid Mech.* **476**, 213–222.

MOHAMED-KASSIM, Z. & LONGMIRE, E. K. 2004 Drop coalescence through a liquid/liquid interface. *Phys. Fluids* **16** (7), 2170–2181.

MONTI, R. & SAVINO, R. 1997 Correlation beween experimenal results and numerical solutions of the Navier–Stokes problem for noncoalescing liquid drops with Marangoni effects. *Phys. Fluids* **9** (2), 260–262.

MONTI, R., SAVINO, R. & CICALA, A. 1996 Surface tension driven-flow in non-coalescing liquid drops. *Acta Astron.* **38** (12), 937–946.

NEITZEL, G. P. & DELL'AVERSANA, P. 2002 Noncoalescence and nonwetting behavior of liquids. *Annu. Rev. Fluid Mech.* **34**, 267–289.

OTTINO, J. M., RANZ, W. E. & MACOSKO, C. W. 1979 A lamellar model for analysis of liquid–liquid mixing. *Chem. Engng Sci.* **34** (6), 877–890.

RANZ, W. E. 1979 Applications of a stretch model to mixing, diffusion, and reaction in laminar and turbulent flows. *AIChE J.* **25** (1), 41–47.

RAYLEIGH, L. 1899 XXXVI. Investigations in capillarity. *Philos. Mag. Ser.* 5 **48** (293), 321–337.

M. Geri, B. Keshavarz, G. H. McKinley and J. W. M. Bush

REYNOLDS, O. 1881 On the floating of drops on the surface of water depending only on the purity of the surface. *Manchester Lit. Phil. Soc. Mem. Proc.* **21**, 1–2.

SAVINO, R., PATERNA, D. & LAPPA, M. 2003 Marangoni flotation of liquid droplets. *J. Fluid Mech.* **479** (March), 307–326.

STEFAN, M. J. 1874 Versuch Uber die scheinbare adhesion. *Sitzungsberichte der Akademie der Wissenschaften in Wien. Mathematik-Naturwissen* **69**, 713–721.

THORODDSEN, S. T. & TAKEHARA, K. 2000 The coalescence cascade of a drop. *Phys. Fluids* **12** (6), 1265–1267.

WALKER, J. 1978 Drops of liquid can be made to float on a liquid. What enables them to do so? *Sci. Am.* 151–158.